UJMR, Conference Special Issue Vol. 10 No. 3. June, 2025, pp. 483 - 494

E-ISSN: 2814 – 1822; P-ISSN: 2616 – 0668

https://doi.org/10.47430/ujmr.25103.046

Received: 15 April 2025 **Accepted:** 14 June 2025

High-Efficiency Nanospheres from Watermelon Rinds for Enhanced Chromium(vi) Bioreduction in Simulated Wastewater and Industrial Effluents

***H. Kassimu[1], H. C. Nzelibe[2], M.T. Isa[3], A. A. Kassimu[4], L.B. Bello[5], A. B. Sallau[2]**

[1]Department of Biochemistry, Faculty of Natural & Applied Science and Agricultural Science, Phoenix University Agwada, Nasarawa State, Nigeria

[2]Department of Biochemistry, Faculty of Life Science, Ahmadu Bello University, Zaria, Kaduna, Nigeria

[3]Department of Chemical Engineering, Faculty of Engineering, Ahmadu Bello University, Zaria, Kaduna, Nigeria

[4]Department of Armament Engineering, Air Force Research and Development Center, Kaduna, Nigeria

[5]Department of Biological Sciences, Faculty of Computing & Applied Sciences, Thomas Adewumi University, Oko, Kwara State, Nigeria

*Correspondence author: habiba.kassimu@phoenixuniversity.edu.ng

Abstract

The bioremediation potentials of Chromium from industrial effluent and simulated wastewater via bioreduction using nanoparticles immobilised watermelon rinds (WMR) were investigated with respect to the effects of process parameters such as concentration of WMR, contact time, temperature, and pH. The kinetics and thermodynamics of the bioreduction process, as well as half-life ($t_{1/2}$) and bioreduction ability of WMR-immobilised nanoparticles. Encapsulation Efficiency and Controlled Release Rate Constants kinetics were studied. Watermelon rinds (WMR) were extracted using the maceration method (70% methanol), encapsulation technique was used for the immobilisation of WMR in the production of nanoparticles, and a batch process was used for the study. Characterisation of the nanoparticles was done using Scanning Electron Microscope (SEM) and Dynamic Light Scattering (DLS). Results showed that bioreduction efficiency was influenced significantly by WMR concentration, as the optimum concentration of 0.1mg/ml was able to reduce 90% of Cr (VI) within a period of 40min, at a temperature of 25 °C and at pH 7.0. The kinetic data showed that the pseudo-second order model best describes the reduction process. Thermodynamic studies showed the values for ΔH^o, ΔG^o, E_a and ΔS^o to be -6500 (J), -10600 (J), 42.24(J/mol) and 25.02 (J/K), respectively, indicating that the bioreduction process was exothermic, feasible and spontaneous. The results also showed that nanoparticles were produced, as evidenced by the DLS spectrum. Encapsulation efficiency of 80.93% was obtained for the nanospheres with released transfer rate constants of 1.61 x 10^{-1} min^{-1}. It can be concluded from the results that nanoparticles immobilised WMR were stable, as they required little or no energy for the bioreduction process. Hence, the stability of the bioactive material (WMR) was necessary for significant bioreduction of Cr (VI).

Keywords: Nanoparticles, Watermelon rinds, Bioreduction, Encapsulation, Efficiency

INTRODUCTION

Improper storage and disposal of Cr(VI)-containing waste have resulted in a huge amount of Cr(VI) flowing into the aquatic and terrestrial habitats, causing a serious environmental health hazard (Kassimu *et al.*, 2022). Tanning industries have been proven to be among the major contributors of heavy metals (Cr, Pb, Zn, Cu, Cd, As, and Se) into water bodies (Ugya *et al.*, 2018). These heavy metals have been demonstrated to be associated with chronic and acute effects on humans and detrimental to other organisms such as algae, plants, animals, and microorganisms (Costa-Boeddeker *et al.*, 2018; Wang *et al.*, 2018; Xun *et al.*, 2018).

Bioreduction involves the process of converting or reducing toxic metals to a less or non-toxic form using bioactive materials (Kassimu *et al.*, 2022). Materials for bioreduction can be produced from many sources, including agro-residue like watermelon rinds (peels/ outer part

E-ISSN: 2814 – 1822; P-ISSN: 2616 – 0668

of watermelon fruits), which are rich in phytochemicals and antioxidants (Kassimu *et al.*, 2022). These materials are readily available and are ecologically and economically friendly (Kassimu *et al.*, 2022). The removal of hexavalent Chromium by reduction can be achieved by chemical or biological methods (Kuppusamy *et al.*, 2016). The chemical methods are not economically or ecologically friendly. Such methods include: reverse osmosis, solvent extraction, chemical precipitation, and ion exchange, which can lead to secondary contamination (Kassimu *et al.*, 2022).

Reductants such as ferrous iron, sulfide, and organic acids naturally existing in environments can directly and effectively reduce Chromium (VI) to (III) (Zhihui *et al.*, 2013). Reduction of Chromium (VI) by microbial enzymes such as chromate reductase reduces toxicity and environmental mobility under both aerobic and anaerobic conditions (Chirwa and Wang 1997). Microorganism reduces Chromium (VI) to (III) intracellularly or by making the extracellular environment more reducing to favour Chromium (VI) reduction (Kuppusamy *et al.*, 2016). The reduction of Chromium (VI) to Chromium (III) is one of the best-used bioreduction strategies, owing to the redox activity of Chromium (Shashi *et al.*, 2017).

Wastewater remediation using nanoparticles is one of the areas of concentration among the various applications of nanotechnology (Suleiman *et al.*, 2015; Yadav *et al.*, 2017). Immobilisation of the bioremediation agent improves its survival, stability, and retention. Immobilisation is slowly gaining importance in wastewater treatment as it delivers better results when compared to the activity of free bioactive materials (Bhaskara and Saha, 2020; Berillo *et al.*,2021). A broad spectrum of immobilisation has been used with various biological/ bioactive materials, including enzymes, cellular organelles, microbial, animal, and plant cells (Bhaskara and Saha, 2020). While bioactive extracts like watermelon rinds show promise in bioremediation, their practical application is often limited by instability under varying conditions, difficulty in recovery/reuse, and potential leaching. Immobilisation within nanoparticles offers a potential solution by enhancing stability, enabling reuse, and facilitating separation. However, efficient encapsulation strategies for complex plant extracts like watermelon rinds and their detailed performance evaluation, particularly for Cr(VI) bioreduction in real effluents, remain underexplored. This study aimed to develop and characterise sodium alginate Nanoparticles (nanospheres) Immobilised Watermelon rind extract (NIW), determine the physicochemical characteristics of NIW, and apply NIW to treat real tannery effluent.

MATERIALS AND METHODS

Sampling and extraction

Watermelons were purchased from a Department of Agronomy farm in Samaru Zaria (11.1607^{0}N, 7.6385^{0}E) and identified at the herbarium unit of the Botany Department, Ahmadu Bello University (ABU) Zaria with a certification/ identification number ABU02234. The method of Kassimu *et al.*, 2022, was adopted for the watermelon rinds. Here, watermelons were cut into pieces, the green rinds were removed, and they were air-dried. All reagents and chemicals used in this study were of analytical grade. This study made use of deionised water throughout the whole experiment. Effluent water, Potassium dichromate [$K_2Cr_2O_7$ (99.5%), Sigma–Aldrich Inc. (St. Louis, MO, USA)], Sulfuric acid [H_2SO_4 (97.0%), sodium alginate (Na-alginate), Calcium carbonate, and paraffin oil.

The dried watermelon rinds (WMR) were pounded into powdered form using a pestle and mortar.

The dried powdered WMR were extracted by cold maceration in 70% methanol by deluging for a day.

Phytochemical Analyses of WMR Extract

Determination of total phenolic contents in the plant extracts

The concentration of phenolics in WMR extract was determined using a spectrophotometric method (Singleton *et al.*, 1999). Methanolic solution of the extract in a concentration of 1 mg/ml was used in the analysis. The reaction mixture was prepared by mixing 0.5 ml of a methanolic solution of WMR extract, 2.5 ml of 10% Folin-Ciocalteu's reagent dissolved in water and 2.5 ml of 7.5% $NaHCO_3$. Blank was concomitantly prepared, containing 0.5 ml methanol, 2.5 ml 10% Folin-Ciocalteu's reagent dissolved in water and 2.5 ml of 7.5% $NaHCO_3$. The WMR extract was thereafter incubated in a thermostat at 45 °C for 45 min. The absorbance was determined using a spectrophotometer at λmax= 765 nm. The WMR extract was prepared

in triplicate, and the mean value of absorbance was obtained. The same procedure was repeated for the standard solution of gallic acid, and the calibration line was construed. Based on the measured absorbance, the concentration of phenolics was read (mg/ml) from the calibration line; then the content of phenolics in extracts was expressed in terms of gallic acid equivalent (mg of GA/g of extract).

Determination of flavonoid concentrations in the plant extracts

The content of flavonoids in the examined plant extracts was determined using a spectrophotometric method (Quettier *et al.*, 2000). The sample contained 1 ml of a methanol solution of the extract in a concentration of 1 mg/ml and 1 ml of 2% AlCl3 solution dissolved in methanol. The samples were incubated for an hour at room temperature. The absorbance was determined using a spectrophotometer at λmax= 415 nm. The samples were prepared in triplicate for each analysis, and the mean value of absorbance was obtained. The same procedure was repeated for the standard solution of rutin, and the calibration line was construed. Based on the measured absorbance, the concentration of flavonoids was read (mg/ml) on the calibration line; then, the content of flavonoids in extracts was expressed in terms of rutin equivalent (mg of RU/g of extract).

Antioxidant Analyses of Watermelon Rinds Extract (WMR)

2,2-diphenyl-1-picrylhydrazyl radical(DPPH) Scavenging Activity:

DPPH scavenging activity of the WMR extract was determined using the method of Upadhyay (2011). Solution of DPPH (0.5 mM) in ethanol was prepared;0.5 mL of WMR (0.02-0.1mg/ml) was added to 1.0 mL of the ethanolic DPPH solution. The mixture was vigorously shaken, left in the dark for 30 min, and the absorbance (at 517 nm) was measured. Scavenging activity was calculated by the following Equation:

%DPPH radical scavenging activity = [(ODC-_ODS) ×100]/ODC 1

Where ODC and ODS are the absorbance of control and test samples, respectively. The results were expressed as IC_{50} values and were calculated by linear regression analysis of tests conducted in triplicate; quercetin was used as positive control.

Superoxide-Radical Scavenging Activity by PMS-NADH (phenyl-methazonium methosulfate-reduced nicotinamide adenine dinucleotide) System: The superoxide radical scavenging ability of the WMR extract was assayed as described by Ao *et al.* (2012). Different concentrations (0.5–5.0 µg/ml) of WMR extract were added to a mixture containing 0.5 mL NADH (105.6 µM) and 0.5 mL NBT (Nitro blue tetrazolium chloride) (66 µM) in 0.1 M phosphate buffer (pH 7.4). The reaction was initiated by the addition of a volume of 0.5 mL of a solution of 15 µM PMS, and after 5 min, the absorbance was measured at 560 nm. The concentration of the test sample required to inhibit NBT reduction by 50 % (IC_{50}) was calculated from the dose-inhibition curve.

Total Antioxidant Activity (TAC): The total antioxidant capacity (TAC) of WMR extract was determined according to the methods of Prieto *et al.* (1999) and Ao *et al.* (2008). Briefly, 0.3 ml of WMR extract (50-100 µg/ml) was mixed with 2.5 ml of phosphomolybdenum reagent (0.6 M sulphuric acid, 28 mM sodium sulphate and 4 mM ammonium molybdate were mixed together in 250 ml deionised water) in test tubes. The tubes were capped and incubated in a boiling water bath at 95 °C for 90 min. After the samples had cooled to room temperature, the absorbance of the reaction mixture was measured after 15 minutes at 695 nm against a blank. Ascorbic acid was used as a standard. A blank was prepared with 2.5 ml regent solution and an appropriate volume of the same solvent (methanol) used for the extraction of WMR extract and it was incubated under the same conditions. Antioxidant capacity was expressed as equivalents of ascorbic acid (standard).

Ferric ion reducing antioxidant power assay (FRAP): Ferric ions reducing power was measured according to the method of Rohan and Anup (2014). watermelon rind (WMR) extract in different concentrations ranging from 100 mg/L to 500 mg/L was mixed with 2.5 ml of 20 mM phosphate buffer and 2.5 ml of 1%(w/v) potassium ferricyanide, and the mixture was incubated at 50 °C for 30 min. Afterwards, 2.5 ml of 10%(w/v) trichloroacetic acid and 0.5 ml 0.1%(w/v) ferric chloride were added to the mixture, which was kept aside for 10 min. Finally, the absorbance was measured at 700 nm. Ascorbic acid was used as a positive reference standard. All assays were run in triplicate and averaged.

Preparation of Nanoparticles Immobilised Watermelon Rinds (NIW)

The encapsulation method was used in the production of nanoparticles immobilised in watermelon rinds as described by Ahmed *et al.* (2013). The principle behind the nanoparticles production is based on an internal gelation technique to obtain homogeneous and more porous nanoparticles. Briefly, 0.2 g of sodium alginate (Na-alginate) was added to 20 mL of deionised water, which was thoroughly stirred and placed on a magnetic stirrer for 5 min. Calcium carbonate (0.2 g) was added to the Na-alginate mixture and stirred for 10 min using a magnetic stirrer. Ten (10) mL of 0.1 mg/ml WMR was added to the mixture (Na and Ca alginate) and stirred for another 10 min, after which 5 mL of 30 % paraffin oil in 1 % span 80 was added and the mixture was stirred thoroughly on a magnetic stirrer for 15 min. 5 mL of glacial acetic acid and 0.2 mL paraffin oil were added to the mixture and stirred for another 20 min to allow for separation. Finally, 1% Tween 80 was used to wash the nanospheres, followed by deionised water. The nanospheres (nanoparticles) were then kept in a sealed bottle in a refrigerator at 4^0C for further use.

Preparation of Simulated Aqueous Solution of Cr (VI) and Sample Collection and Characterisation of Tannery Effluent

Hexavalent chromium Cr (VI) stock solution (1000 mg/L) was made by weighing 2.829 g of potassium dichromate in a measuring cylinder containing 1000 mL of deionised water. 10 mg /L solution was then prepared from the stock solution with water (deionised) (Poojari *et al.*, 2015).

The tannery effluent samples were collected in sterilised containers placed in a flask containing an ice block from Sharada Industrial Area (11.9739° N, 8.5089° E) of Kano State, Nigeria, and were examined to estimate the amount of pollutants as well as heavy metals like Cr (VI) in the water sample.

Concentration Estimation of Cr (VI) in Tannery Effluent

Hexavalent Chromium was estimated spectrophotometrically using 1,5-diphenylcarbazide (DPC) as described by Shugaba *et al.* (2012). One millilitre (1 mL) of 0.2 % (w/v) of 1,5-diphenylcarbazide solution (prepared in 95% ethanol and 1 mL of H_2SO_4) was added to 1 mL of the sample solution. The solution was allowed to stand for 10 min, after which the absorbance was read against a reagent blank at 540 nm.

Characterisation of the Nanoparticle Immobilised Watermelon Rinds (NIW)

To know the particle size distribution, the NIW were suspended in deionised water for 1 h to prevent the agglomeration of particles and to evenly disperse the nanoparticles in the sample. The sample (nanoparticles immobilised WMR suspended in deionised water (2 mL each) was pipetted into a quartz cuvette, then particle size distribution (PSD) and the polydispersity index (PDI) were measured using the dynamic light scattering (Malvern Zetasizer ZS90). The instrument was pre-programmed to take three consecutive readings by intensity and volume, and each sample was measured in triplicate.

Encapsulation efficiencies were determined as a function of the decreased DPPH concentration over time (Kassama and Misir 2017). NIW were placed in a beaker containing 3 mL of 10 mg/ml of Cr (VI) solution separately, and 3 mL of 0.1 mg/ml DPPH was added, allowed to stand for 50 min at room temperature for proper diffusion of the NIW. A control was also set up containing 3 mL of Cr (VI) solution and 3 mL of DPPH. Absorbance was taken at 517 nm after 50 min. The Encapsulation Efficiencies (EE) was calculated using the formula:

Encapsulation Efficiency (%)= [Actual weight of NIW/ Theoretical Weight of NIW] x 100 (1)

The Control Release Kinetics of the NIW was carried out as described by Kassama and Missir (2017), and was used with slight modification. Briefly, 0.1 mg/mL of the NIW was added to 3 mL of 0.1 mM DPPH solution. The reduction of the DPPH concentration was observed over time relative to the NIW of the same concentration. The absorbance was measured at 517 nm as the DPPH concentration decreased. The release kinetics were then estimated based on the decrease in DPPH, which was inversely proportional to the release of the bioactive components from NIW that reacted with the DPPH solution. The rate constant was determined by applying the following Equation (2):

$$In\left(\frac{A-A_0}{A_0-A_\infty}\right) = Kt \quad (2)$$

Where A is the absorbance at time t, A_0 is the absorbance at time 0, Aα is the final absorbance, and K is the release rate constant of the bioactive component.

Effect of Process Parameters on Cr (VI) Bioreduction

The effect of contact time on bioreduction of hexavalent Chromium by NIW bioreductant in aqueous solution of Cr (VI) (10 mg/L) was done by changing (10 - 80 min) the time of the reaction process. pH was adjusted to 7.0 using hydrochloric acid (0.1 M) and sodium hydroxide (0.1 M) solutions, at a temperature of 25 ^{0}C and chromium (VI) concentration in solution was analysed spectrophotometrically and absorbance was read at 540nm.

Effect of Concentration of NIW

To examine the effect of NIW concentration, varying concentrations of NIW (0.1–1 mg/mL) were prepared. The effect of these concentrations was tested using 4 mL of an aqueous Cr(VI) solution (10 mg/L) at room temperature (25 °C), with the pH adjusted to 7.0 using 0.1 M hydrochloric acid and 0.1 M sodium hydroxide solutions. Each reaction mixture was allowed to stand for 40 minutes, after which the Cr(VI) concentration was determined spectrophotometrically, and the absorbance was measured at 540 nm.

The effect of pH on the bioreduction of Cr (VI) was carried out by changing the pH of the reaction mixture between 2, 7 and 12 (at an interval of 5) so as to examine the effects of different pH on the bioreduction of hexavalent Chromium to trivalent Chromium. The reaction mixtures were incubated at the optimum contact time (40 min), and at room temperature (25 ^{0}C). Chromium in the solution was analysed spectrophotometrically, and absorbance was read at 540nm.

The effect of temperature on Cr (VI)bioreduction by NIW was investigated using batch experimentation by treating 4mL of 10 mg/L of Cr (VI) with 1mL of 0.1 mg/mL of NIW in a well-covered 10 mL test tube at varying temperatures (25 - 65 °C) in a water bath. This was done at 10 °C increments under optimum pH (7.0) and contact time of 40 min. The chromium concentration was analysed spectrophotometrically, and absorbance was read at 540nm.

RESULTS

Table 1.0 shows the phytochemicals found in watermelon rinds. It is seen that watermelon is very rich in phytochemicals like: Flavonoid (41.07 ± 1.09), phenol (33.43 ± 0.00), Alkaloid (21.13 ± 1.00) and flavonols(25.00 ± 0.02). Table 2.0 shows the result of the antioxidants analyses of Watermelon Rinds (WMR) extract. From the table, it can be seen that the IC_{50}(µg/ml) for DPPH, H_2O_2, and TAC were 34.10 ± 1.00, 23.03± 0.22and 35.63 ± 1.03, while the FRAP (µg / mg sample) activity was 17.01± 0.14. These observations show that watermelon rinds are rich in antioxidants.

Figure 1 shows the dynamic light scattering spectrum (DLS) of the NIW. The figure shows that nanoparticles of watermelon rinds were produced, and the sizes of these particles lie between the nanorange (15nm-100nm). Table 3.0 shows the presence of other metals aside from Chromium found in the tannery effluents. Tale 4.0 shows the physicochemical characteristics of Tannery Effluent. From the table, it is seen that the appearance of the effluent was dark brown in colour, having a pH of 3.6, and highly polluted. Table 5.0 shows the characteristics of the nanoparticles produced. It can be deduced from the tables that the nanospheres produced were spherical in shape with an encapsulation efficiency of 80.93%. Table 6.0 shows the kinetic and thermodynamic parameters of the bioreduction process. From the experiment conducted, the correlation coefficient (R^2) value at pH 7. For pseudo-first-order was 0.76, while that of pseudo-second order was 0.99, respectively. To describe the thermodynamic behaviour of Cr (VI) bioreduction by NIW, relevant parameterssuch asArrhenius activation energy (Ea), changes in activation enthalpy (ΔH), entropy (ΔS), and Gibbs free energy (ΔG) were calculated. The summary of thermodynamic parameters for the bioreduction process is also shown in Table 6.0. The characterisation of the NIW produced was carried out by SEM and DLS. It can be deduced that the NIWs are polydispersed and stable, hence the bioreduction potentials. The SEM analysis confirmed the presence of nanoparticles.

The amount of WMR immobilised in the nanoparticles (nanospheres) is the Encapsulation Efficiency (EE), which was determined and calculated using Equation 1.

Figures 4 show the effect of contact time in Cr (VI) bioreduction both in simulated water and industrial effluent. It is revealed from the Figures that the optimum contact time for the bioreduction process was 40 min since 78% (simulated water) and 93% (tannery effluent) of Cr (VI) were bioreduced by NIW at 40min.

Similarly, the optimum temperature for the bioreduction of Cr (VI) by NIW, both in simulated water and tannery effluent, was 25 °C as seen in Figure 7.0. This figure shows that when the temperature was 5 °C -25 °C, a significant effect on the bioreduction of Cr (VI) was observed, as over 94% (simulated water) and 68% (tannery effluent) reduction in the efficiency was achieved at 25 °C. Also, Cr (VI) bioreduction in both simulated water and industrial effluent by NIW was best at pH 7.0, which is the optimum pH for the bioreduction process as shown in Figure 6, as 98% of Cr (VI) in simulated water and 69% of Cr (VI) in industrial effluent were reduced at pH 7. Finally, the concentration of NIW for the bioreduction process was inversely proportional to the concentration of Chromium (VI) in solution, as seen in Figure 5.

Table 1.0: Phytochemical Analyses of Watermelon Rind (WMR)

Analyte	Mean ± SD
Flavonoid (mg RU/g extract)	41.07 ± 1.09
Phenol (mg catechol equivalent/g dry material)	33.43 ± 0.00
Alkaloid (mg quercetin/g dry material)	21.13 ± 1.00
Flavonols (mg quercetin/g dry material)	25.00 ± 0.02

n=3

Table 2.0Mean Antioxidant Activity of Watermelon Rind (WMR)

Analyte	Mean ± SD
DPPH, IC_{50} (µg/ml)	34.14 ± 1.00
H_2O_2, IC_{50} (µg/ml)	23.03 ± 0.22
TAC, IC_{50} (µg/ml)	39.36 ± 1.03
FRAP (µg/mg)	17.10 ± 0.14

n=3

Table 3.0Determination of Heavy Metal Contents of Tannery Wastewater

Metal	Tannery Effluent (mg/L) ± SD
Cr	5.74 ± 1.00
Pb	1.19 ± 0.16
Cd	0.75 ± 0.23
Cu	0.23 ± 0.17
Fe	3.04 ± 0.44
Hg	1.22 ± 0.28
Mn	0.042 ± 1.02
Ni	0.48 ± 0.00
Co	0.05 ± 0.32
Zn	2.75 ± 0.43

Table 4.0 Physicochemical Characteristics of TanneryEffluent

Property	Tannery Effluent
pH	3.6
Appearance	Dark
Dissolved Oxygen (mg/L)	3.29
Biological Oxygen Demand (BOD) (mg/L)	875
Chemical Oxygen Demand (COD) (mg/L)	1,037

E-ISSN: 2814 – 1822; P-ISSN: 2616 – 0668

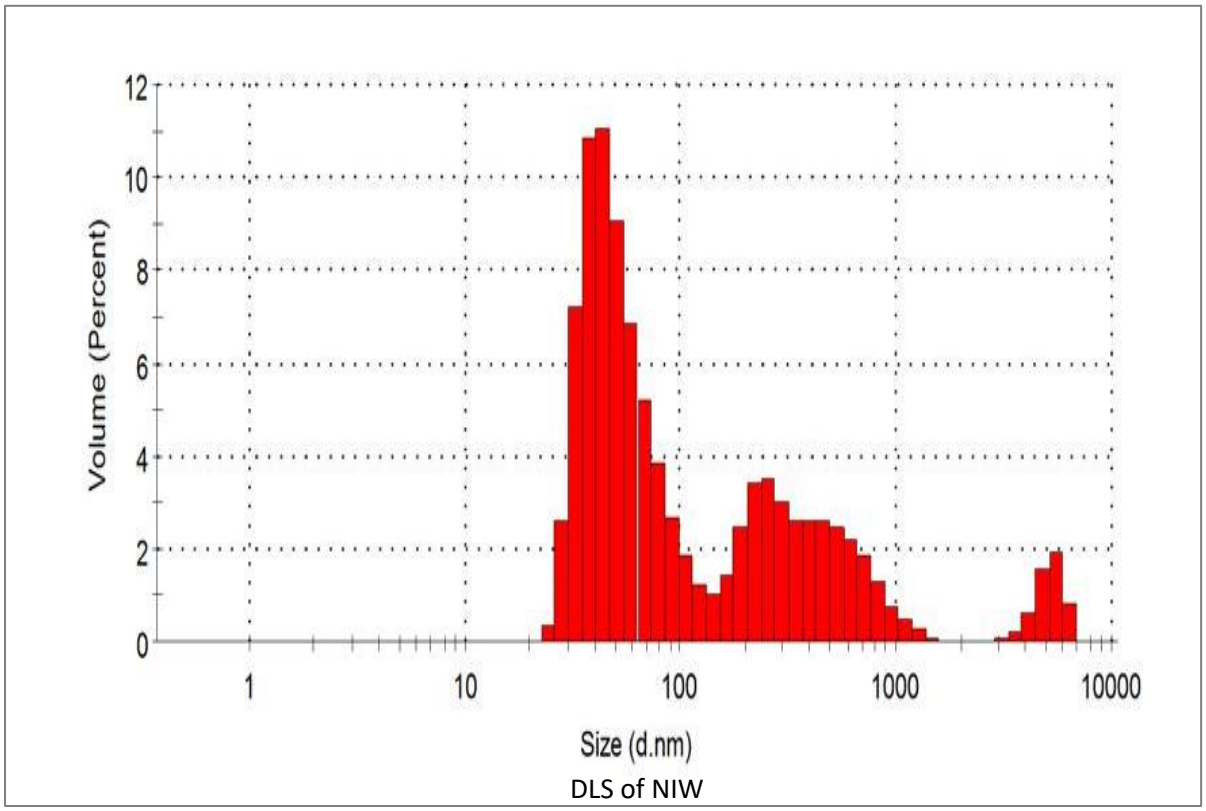

Fig. 1 Dynamic Light Scattering Spectrum of NIW Showing Size Distribution by Volume.

Plate 1: SEM Analysis of Nanoparticles Immobilized Watermelon Rinds

E-ISSN: 2814 – 1822; P-ISSN: 2616 – 0668

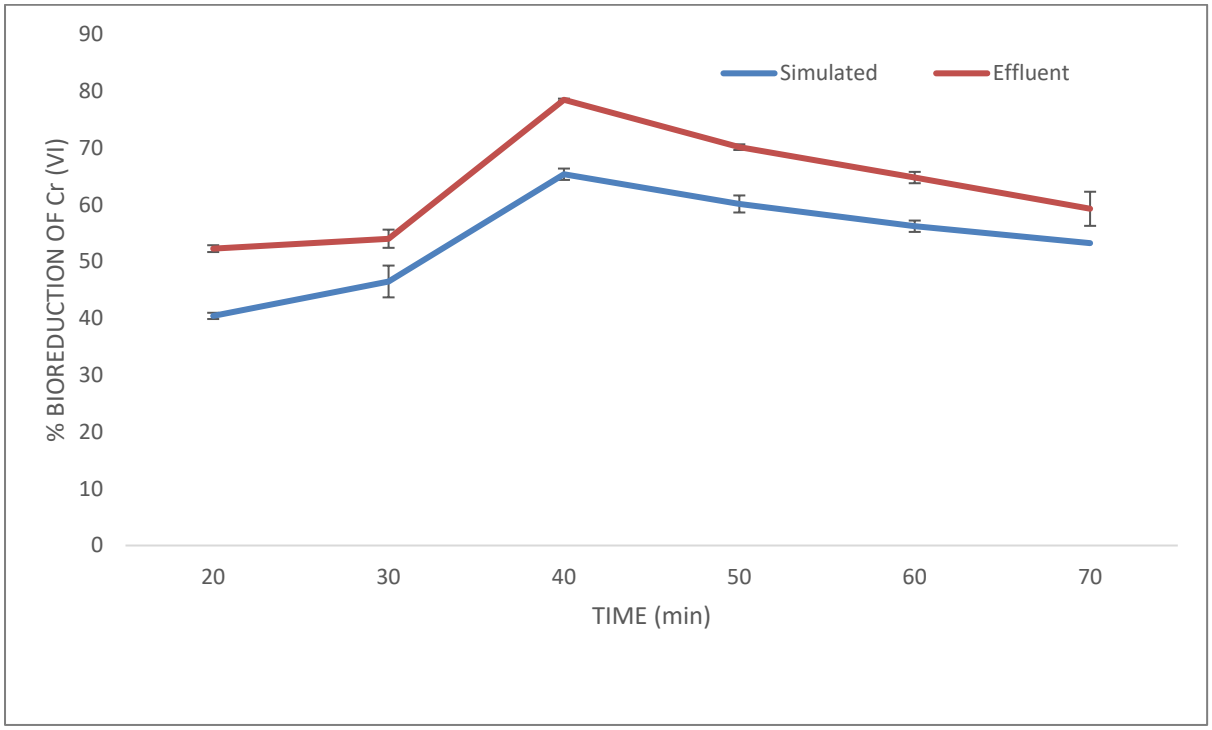

Fig.4 Effect of Time on Cr (VI) Bioreduction process.

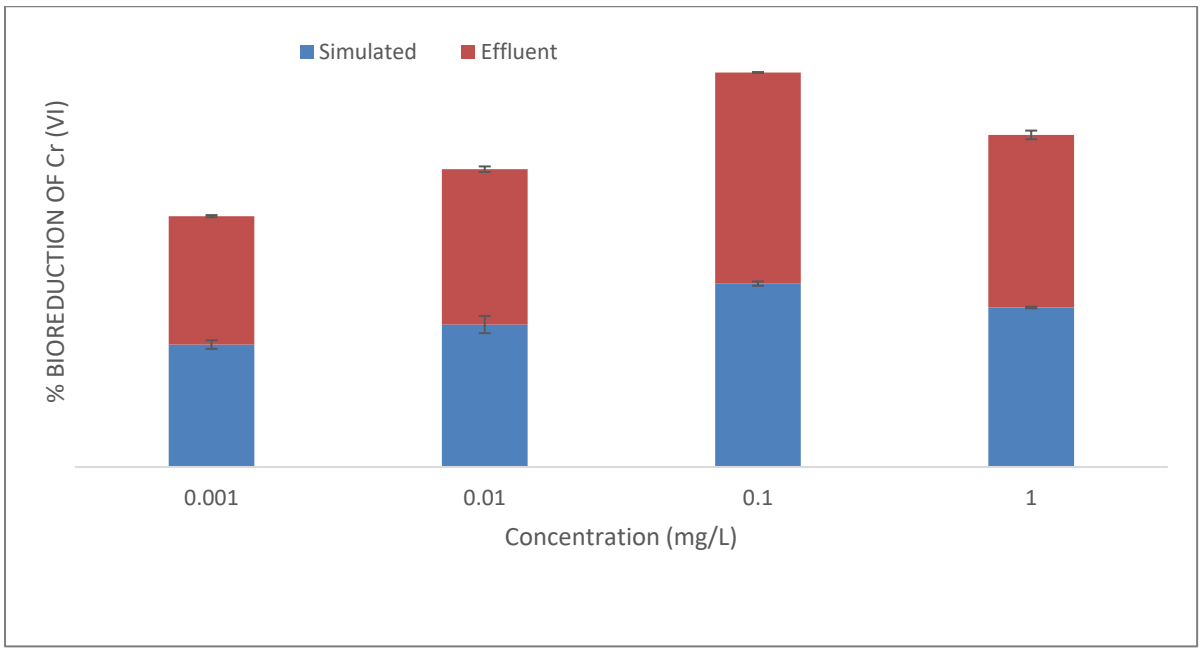

Fig.5 Effect of NIW Concentration on Cr (VI) Bioreduction Process.

Table 5.0 Physicochemical Characteristics of NIW

Characteristics	Result
Appearance/Morphology	Spherical
Average Diameter (μm)	$3.42 \times 10^{-3} \pm 0.00$
Volume (cm^3)	$1.68 \times 10^{-7} \pm 0.00$
Pore Size (μm)	0.23 ± 0.00
$t_{1/2}(min^{-1})$	2.02 ± 1.12
Encapsulation Efficiency (%)	80.93 ± 0.01
Controlled Release Transfer Rate Constant (min^{-1})	1.61×10^{-1}
R^2	0.91

E-ISSN: 2814 – 1822; P-ISSN: 2616 – 0668

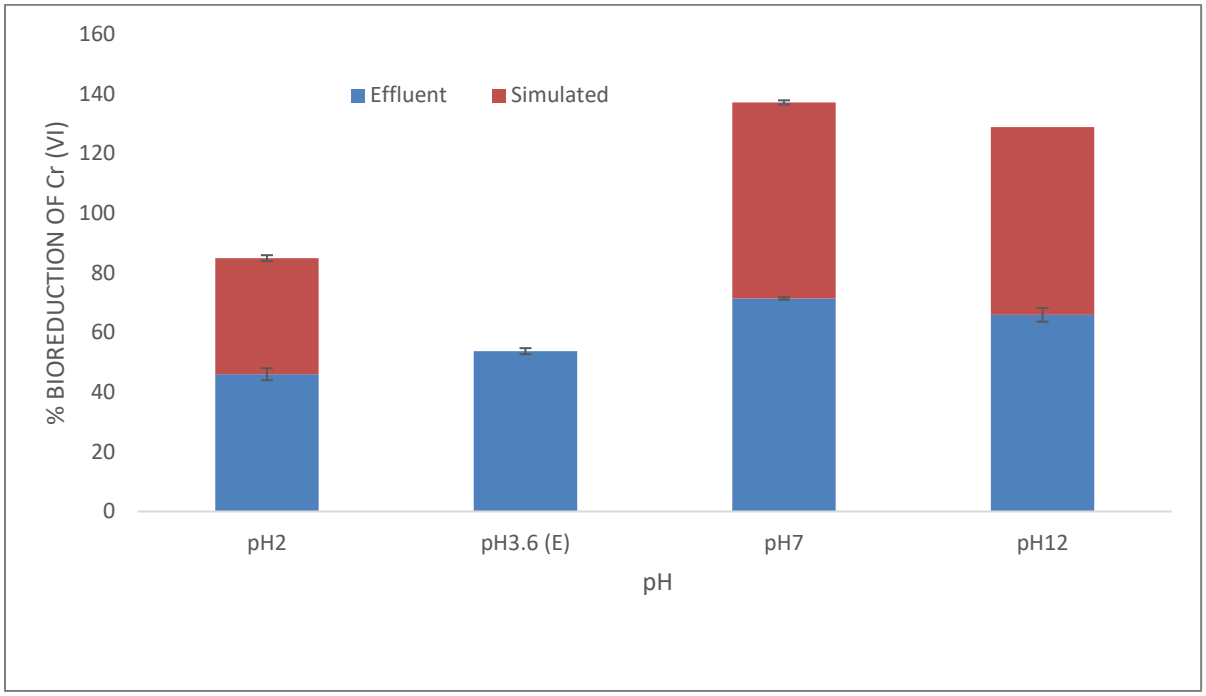

Fig.6 Effect of pH on Cr (VI) Bioreduction process.

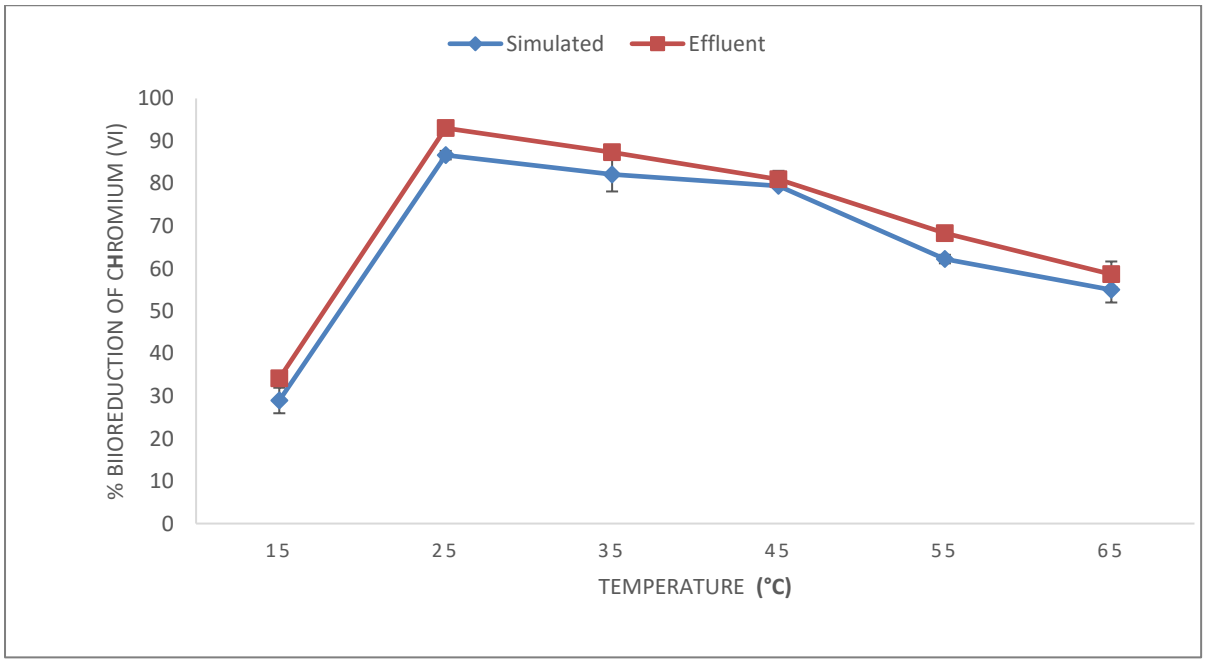

Fig.7 Effect of Temperature on Cr (VI) Bioreduction process.

DISCUSSION

Phytochemical analyses of WMR extract show the presence of flavonoids, Alkaloids, phenols and flavonols in the WMR extract. The antioxidant activity assessments of WMR were done by measuring the TAC and FRAP activities and its capacity to scavenge the DPPH and superoxide anion radicals. The results showed that WMR exhibits high antioxidant and free radical scavenging activities. It also chelates iron andh as high reducing power. This study indicates that WMR is a significant source of natural antioxidant, hence its bioreduction potential of Cr (VI).

The hydrodynamic particle size and size distribution, as well as the Polydispersity Index (PDI) of NIW were determined by DLS, as shown in Figure 1. The result showed that 61.22% of the NIW produced lie between 15-100nm, showing that the produced Nanoparticles

E-ISSN: 2814 – 1822; P-ISSN: 2616 – 0668

belonged to the nano range (Li *et al.*, 2021), polydispersity index (PDI) of the nanospheres was 0.30. The PDI values explained that the NIW are polydisperse, and the zeta potential (21mV) shows that NIW is stable. The zeta potentials revealed that the immobilised delivery systems were charged, thus, did not form aggregates, which led to their stability, hence, the bioreduction potentials, as shown in Table 7.0. SEM analysis revealed that the nanoparticles produced were morphologically spherical, as seen in Plate 1.

Table 6.0 Kinetics and Thermodynamics Results

Characteristics	Result
Thermodynamic Parameters	
ΔH^0 (J)	-6500
ΔS^0 (J/K)	20.00
Ea (J/mol)	7.00
ΔG^0 (J)	-10.60
Pseudo-first-order Kinetics	
q_e (mg/mL)	0.04
K_1 (mg/mL/min)	0.86
R^2	0.78
Pseudo-second-order Kinetics	
q_e (mg/mL)	11.33
K_2 (mg/mL/min)	18.10
R^2	0.99

Table 7.0: Dynamic Light Scattering (DLS)

Characteristics	Result
Z-Average (d·nm)	61.09
Zeta potential (mV)	21
PDI	0.30

The EE of the nanoparticles was 80.93%. This shows that 80.93% of the extracted WMR was used in the production of NIW. This value is much higher than that reported by Hill *et al.* (2013), (48% and 39%), Alam *et al.* (2012) (63%) and Kassama and Missir(2017), (63% forliquid gel(LG). Also, the value is lower than that reported by Kassama and Missir (2017) (87%) for freeze-dried powdered gel (FDG) and Odeh et al. (2012) (90%), respectively. This may be due to the method of immobilisation. The rate constant of the NIW was 1.61 x 10^{-1} min^{-1} as seen in Table 4.0. The rate constant kinetics showed the rate at which the bioactive compound diffuses out of the NIW for the bioreduction process. This was manifested by impeding the mass transfer of the DPPH, thereby providing a longer release time (Kassama and Missir 2017). The rate constant kinetics also showed that the antioxidant properties of NIW are efficient after immobilisation.

In order to evaluate the kinetic parameters, pseudo-first-order and pseudo-second-order models were tested to analyse the kinetics of the bioreduction process. Both kinetic models have been used to understand the bioremediation kinetics and the correlation coefficient, R^2 (Mekonnen *et al.*, 2015). However, the correlation coefficient, R^2, values showed that the pseudo-second-order model fits better to the experimental data better than the pseudo-first-order model. Thus, the Pseudo second order model assumes that the rate of reduction of solute (Cr (VI) is proportional to the available sites on the bioreductant (NIW). The thermodynamics results showed that the bioreduction of Cr(VI) by ARE is spontaneous, exothermic and feasible; this is because the values of ΔG° and ΔH° were negative and ΔS° was positive (Bayazit and Kerkez, 2014). This means that as the Cr(VI) was reduced by the bioactive compounds present in NIW, the degree of randomness was increased, and the process does not need heat as well as energy (E_a) before proceeding to completion within the optimum period. As seen in Table 5.0.

Zeraatkar *et al.* (2016) explained that the influence of temperature on bioreduction processes depends upon its nature. In endothermic processes, an increase in temperature leads to an increase in reaction, while an increase in temperature decreases the reaction of a bioremediation process in the case of exothermic processes. This study showed that the bioreduction of Cr (VI) by NIW was an exothermic process. In Cr (VI) simulated wastewater and industrial effluent, bioreduction of Cr (VI) took place at neutral pH (7), as over 80 % of the Cr (VI) was reduced in 40 min by NIW. Thus, the performance of the tannery effluent is higher than that of the simulated wastewater. This may be a result of a concentration difference.

CONCLUSION

This study shows that NIW offers a promising, energy-efficient strategy for Cr(VI) remediation in wastewater, leveraging agricultural waste.

CONFLICT OF INTEREST

The authors declare no conflict of interest.

RECOMMENDATIONS

We recommend that these findings should be applied in industries before the release of tannery effluent in the environment in order to reduce or bioremediate heavy metals pollution, especially Chromium (VI), from the environment.

ACKNOWLEDGEMENTS

The authors wish to thank God and all those who supported us, most especially AVM A.A. Kassimu (RTD) for his generosity.

REFERENCES

Ahmed, M. M., Abd El Rasoul, S., Auda, S. H., & Ibrahim, M. A. (2013). Emulsification/internal gelation as a method for preparation of diclofenac sodium-sodium alginate microparticles. *Saudi Pharmaceutical Journal, 21*, 61–69. [Crossref]

Alam, S., Mustafa, G., Khan, Z. I., Islam, F., Bhatnagar, A., Ahmad, F., & Kumar, M. (2012). Development and evaluation of thymoquinone-encapsulated chitosan nanoparticles for nose-to-brain targeting: A pharmacoscintigraphic study. *International Journal of Nanomedicine, 7*, 5705–5718. [Crossref]

Ao, C., Higa, T., Khanh, T. D., Upadhyay, A., & Tawata, S. (2012). Antioxidant phenolic compounds from *Smilax sebeana* Miq. *LWT-Food Science and Technology, 44*, 1681–1686. [Crossref]

Ao, C., Li, A., Elzaawely, A. A., Xuan, T. D., & Tawata, S. (2008). Evaluation of antioxidant and antibacterial activities of *Ficus microcarpa* L. fil. extract. *Food Control, 19*, 940–948. [Crossref]

Bayazit, A. S., & Kerkez, Ö. (2014). Hexavalent chromium adsorption on superparamagnetic multiwalled carbon nanotubes and activated carbon composites. *Chemical Engineering Research and Design, 92*(8), 1495–1503. [Crossref]

Berillo, D., Al-Jwaid, A., & Caplin, J. (2021). Polymeric materials used for immobilisation of bacteria for the bioremediation of contaminants in water. *Polymers, 13*, 1073. [Crossref]

Bhaskara Rao, K. V., & Saha, P. (2020). Immobilisation as a powerful bioremediation tool for abatement of dye pollution: A review. *Environmental Reviews*, 1–74.

Chirwa, E. M. N., & Wang, Y. T. (1997). Hexavalent chromium reduction by *Bacillus* sp. in a packed-bed bioreactor. *Environmental Science & Technology, 31*(5), 1446–1451. [Crossref]

Costa-Boeddeker, S., Le Xuan, T., Hoelzmann, P., de Stigter, H. C., van Gaever, P., & Hoang Duc, H. (2018). The hidden threat of heavy metal pollution in high sedimentation and highly dynamic environment: Assessment of metal accumulation rates in the Thi Vai Estuary. *Environmental Pollution, 242*, 348–356. [Crossref]

Hill, L. E., Taylor, T. M., & Gomes, C. (2013). Antimicrobial efficacy of poly (DL-lactide-co-glycolide) (PLGA) nanoparticles with entrapped cinnamon bark extract against *Listeria monocytogenes* and *Salmonella typhimurium*. *Journal of Food Science, 78*(4), N626–N632. [Crossref]

Kassama, L. S., & Misir, J. (2017). Physicochemical properties and control release of *Aloe vera* (*Aloe barbadensis* Miller) bioactive loaded poly (lactic co-glycolide acid) synthesised nanoparticles. *Advances in Chemical Engineering and Science, 7*, 333–348. [Crossref]

Kassimu, H., Sallau, A. B., Nzelibe, H. C., & Isa, M. T. (2022). Hexavalent chromium (Cr VI) bioreduction potential of anthocyanins-rich extract of watermelon (*Citrullus lanatus*) rind. *Chemistry Africa*. [Crossref]

Kuppusamy, S., Kadarkarai, M., Giovanni, B., Akon, H., & Aruliah, R. (2016). Bioreduction of hexavalent chromium by *Pseudomonas stutzeri* L1 and *Acinetobacter baumannii* L2. *Annals of Microbiology, 67*, 91–98. [Crossref]

Li, X., Fan, M., Zhang, Y., Liu, L., Yi, F., Chang, J., & Li, J. (2021). Remediation of chromium- and fluoride-contaminated groundwater by immobilised *Citrobacter* sp. on a nano ZrO2 hybrid material. *PLoS ONE, 16*(6), e0253496. [Crossref]

Mekonnen, E., Yitbarek, M., & Soreta, T. R. (2015). Kinetic and thermodynamic studies of the adsorption of Cr (VI) onto some selected local adsorbents. *South African Journal of Chemistry, 68*, 45–52. [Crossref]

Odeh, F., Ismail, S. I., Abu-Dahab, R., Mahmoud, I. S., & Al-Bawab, A. (2012). Thymoquinone in liposomes: A study of loading efficiency and biological activity

towards breast cancer. *Drug Delivery, 19*(5), 371–377. [Crossref]

Poojari, A. C., Maind, S. D., & Bhalerao, S. A. (2015). Effective removal of Cr (VI) from aqueous solutions using rind of orange (*Citrus sinensis* (L.) Osbeck). *International Journal of Current Microbiology and Applied Sciences, 4*(4), 653–671.

Prieto, P., Pineda, M., & Aguilar, M. (1999). Spectrophotometric quantitation of antioxidant capacity through the formation of a phosphomolybdenum complex: Specific application to the determination of vitamin E. *Analytical Biochemistry, 269*, 337–341. [Crossref]

Quettier, D. C., Gressier, B., Vasseur, J., Dine, T., Brunet, C., Luyckx, M. C., Cayin, J. C., Bailleul, F., & Trotin, F. (2000). Phenolic compounds and antioxidant activities of buckwheat (*Fagopyrum esculentum* Moench) hulls and flour. *Journal of Ethnopharmacology, 72*, 35-42. [Crossref]

Rohan, S. P., & Anup, S. H. (2014). Total antioxidant capacity (TAC) of fresh leaves of *Kalanchoe pinnata*. *Journal of Pharmacognosy and Phytochemistry, 2*(5), 32–35.

Shashi, P. D., Mika, S., & Rajender, S. V. (2017). Reduction of hexavalent chromium using *Sorbaria sorbifolia* aqueous leaf extract. *Applied Sciences, 7*(7), 715. [Crossref]

Shugaba, A., Buba, F., Kolo, B. G., Nok, A. J., & Ameh, D. A. (2012). Uptake and reduction of hexavalent chromium by *Aspergillus niger* and *Aspergillus parasiticus*. *Journal of Petroleum and Environmental Biotechnology, 3*(3), 119. [Crossref]

Singleton, V. L., Orthofer, R., & Lamuela-Raventos, R. M. (1999). Analysis of total phenols and other oxidation substrates and antioxidants by means of Folin-Ciocalteu reagent. *Methods in Enzymology, 299*, 152–178. [Crossref]

Suleiman, M., Mousa, M., & Hussein, A. I. A. (2015). Toxic chromium removal by bacterial strain. *Journal of Materials and Environmental Science, 6*(7), 1924-1937.

Ugya, A. Y., Hua, X., & Ma, J. (2018). Biosorption of Cr^{3+} and Pb^{2+} from tannery wastewater using combined fruit waste. *Applied Ecology and Environmental Research, 17*(2), 1773–1787. [Crossref]

Upadhyay, A., Chompoo, J., Araki, N., & Tawata, S. (2011). Antioxidant, antimicrobial, 15-LOX, and AGEs inhibitions by pineapple stem waste. *Journal of Food Science, 76*(9), C9–C15. [Crossref]

Wang, M., Nishihama, R., Onishi, M., & Pringle, J. R. (2018). Role of the Hof1–Cyk3 interaction in cleavage-furrow ingression and primary-septum formation during yeast cytokinesis. *Molecular Biology of the Cell, 29*(5), 597–609. [Crossref]

Xun, Z., Can, J., Yuliang, J., Guifeng, L., Guomin, W., & Zhenwu, K. (2018). A novel gallic acid-grafted-lignin biosorbent for the selective removal of lead ions from aqueous solutions.

Yadav, K. K., Singh, J. K., Gupta, N., & Kumar, V. (2017). A review of nano-bioremediation technologies for environmental cleanup: A novel biological approach. *Journal of Materials and Environmental Sciences, 8*(2), 740–757.

Zeraatkar, A. K., Ahmadzadeh, H., Talebi, A. F., Moheimani, N. R., & McHenry, M. P. (2016). Potential use of algae for heavy metal bioremediation, a critical review. *Journal of Environmental Management, 181*, 817–831. [Crossref]

Zhihui, X., Bai, S., Liang, J., Zhou, L., & Lan, Y. (2013). Photocatalytic reduction of Cr(VI) by citric and oxalic acids over biogenetic jarosite. *Materials Science and Engineering C, 33*(4), 2192–2196. [Crossref]